The EMBO Journal vol.4 no.3 pp.829–835, 1985

The solution structure of a B-DNA undecamer comprising a portion of the specific target site for the cAMP receptor protein in the *gal* operon. Refinement on the basis of interproton distance data

G.Marius Clore and Angela M.Gronenborn

Max-Planck-Institut für Biochemie, D-8033 Martinsried bei München, FRG

Communicated by R. Huber

A restrained least squares refinement of the solution structure of the double-stranded DNA undecamer 5′d(AAGTGTGACAT).5′d(ATGTCACACTT) comprising a portion of the specific target site of the cAMP receptor protein in the *gal* operon is presented. The structure is refined on the basis of both distance and planarity restraints, 2331 in all. The distance restraints comprise 150 interproton distances determined from pre-steady state nuclear Overhauser enhancement measurements and 2159 other interatomic distances derived from idealized geometry (i.e., distances between covalently bonded atoms, between atoms defining fixed bond angles, and between atoms defining hydrogen bonding in AT and GC base pairs). Two refinements were carried out and in both cases the final RMS difference between the experimental and calculated interproton distances was 0.2 Å. The difference between the two refined structures is small (overall RMS difference of 0.23 Å) and represents the error in the refined coordinates. Although the refined structures have an overall B-type conformation there are large variations in many of the local conformational parameters including backbone and glycosidic bond torsion angles, helical twist and propellor twist, base roll and base tilt angles.

Key words: B-DNA/solution structure/NOE/interproton distances/refinement/local structure/CRP

Introduction

Using pre-steady proton-proton nuclear Overhauser enhancement (NOE) measurements we have recently presented the assignment of proton resonances and the low resolution solution structure of the double-stranded B-DNA undecamer

5′ d A_1 A_2 G_3 T_4 G_5 T_6 G_7 A_8 C_9 A_{10} T_{11} strand 1
3′ d T_{22} T_{21} C_{20} A_{19} C_{18} A_{17} C_{16} T_{15} G_{14} T_{13} A_{12} strand 2

(Clore and Gronenborn, 1984a), as well as measurements of internal mobility and interproton disances (Clore and Gronenborn, 1984b, 1984c). This undecamer comprises a portion of the specific DNA target site for the cAMP receptor protein of *Escherichia coli* (CRP, also known as catabolite activator protein or CAP) in the gal operon (Taniguchi *et al.*, 1979) and contains eight base pairs out of the 10-bp concensus sequence 5′d (AA-TGTGA--T----CA) making up specific CRP sites (Ebright, 1982). Here we present a restrained least squares refinement of the solution structure of the DNA undecamer on the basis of the interproton distances previously determined from NOE measurements (Clore and Gronenborn, 1984c).

The single crystal structure of the B-DNA dodecamer 5′d $(CGCGAATTCGCG)_2$ demonstrated that B-DNA is not a regular helix but exhibits local structural variations (Dickerson and Drew, 1981). Clearly sequence-specific variations in nucleotide structure can play an important role in specific DNA-protein interactions. It is therefore the aim of this study to explore the type, extent and potential sequence specificity of local structural variations in the B-DNA undecamer in solution and to examine how these variations relate to those observed in the crystal structure of the B-DNA dodecamer.

Results and Discussion

Refinement

Obtaining the three dimensional structures of proteins and oligonucleotides in solution has long been a goal of NMR spectroscopists. However, it is only in recent years that considerable progress has been made in this area. The task of solving the three dimensional structures of macromolecules in solution by NMR proceeds in three stages, two of which have already been accomplished in the case of the B-DNA undecamer (Clore and Gronenborn, 1984a, 1984c). The first stage involves the sequential assignment of proton resonances through the combined use of through bond and through space (<5 Å) connectivities. This was pioneered by Wüthrich and his collaborators in the case of proteins (Wagner *et al.*, 1981; Wagner and Wüthrich, 1982a, 1982b; Wüthrich *et al.*, 1982; Štrop *et al.*, 1983; Williamson *et al.*, 1984) and analogous procedures were later devised for oligonucleotides by a number of groups simultaneously (Clore and Gronenborn, 1983, 1984a; Clore *et al.*, 1984; Gronenborn *et al.*, 1984; Gronenborn and Clore, 1984; Reid *et al.*, 1983a; 1983b; Weiss *et al.*, 1984; Hare *et al.*, 1983; Haasnoot *et al.*,

Table I. RMS difference (Å) between the target distance restraints and the corresponding calculated distances in the initial B-DNA model[a] and the final refined structures I and II of the DNA undecamer

	Number of restraints	RMS difference (Å) Initial B-DNA model[a]	Final refined structures I	II
All distances				
r<2.12 Å	1076	0.107	0.034	0.030
2.12 Å < r<2.6 Å	1085	0.132	0.052	0.047
r>2.6 Å	148	0.495	0.194	0.190
Planes[b]	22	0.003	0.014	0.014
Interproton distances[c]	150	0.642	0.200	0.193
Total number of atoms:	700 (2094 degrees of freedom)			
Total number of restraints:	2331			
Overall RMS shifts:				
initial structure *versus* refined structure I:				0.72 Å
initial structure *versus* refined structure II:				0.71 Å
refined structure I *versus* refined structure II:				0.23 Å

[a]Derived from the fibre diffraction data of Arnott and Hukins (1973).
[b]For each residue the C1′-atom of the deoxyribose and all the atoms of the base (with the exception of the methyl protons) are constrained to lie in the same plane.
[c]These interproton distances are those determined by Clore and Gronenborn (1984c) using pre-steady state NOE measurements. They do not include interproton distances which are fixed by the geometry of the sugar ring and bases themselves.

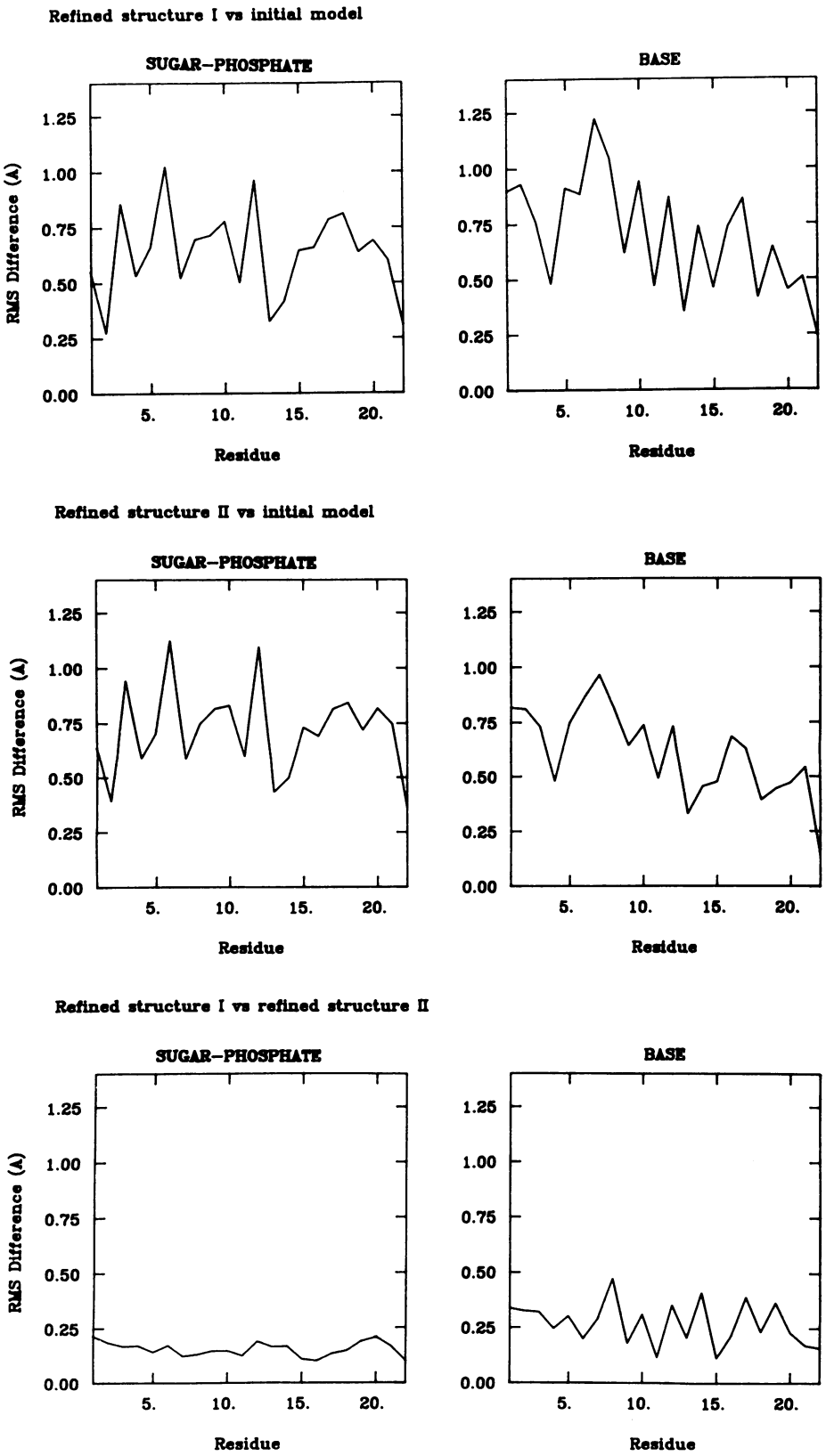

Fig. 1. Variations in RMS difference for the sugar-phosphate and base moieties between the initial B-DNA model, refined structure I and refined structure II of the undecamer as a function of residue number.

1983; Scheek *et al.*, 1984; Feigon *et al.*, 1983). The second stage involves determining interproton distances through the use of pre-steady state NOE measurements (Wagner and Wüthrich, 1979; Dobson *et al.*, 1982; Keepers and James, 1984; Clore and Gronenborn, 1985). The third stage involves the determination of the three-dimensional structure of the macromolecule on the basis of the interproton distance data. This final step can be tackled in a number of ways. One approach involves the *ab initio*

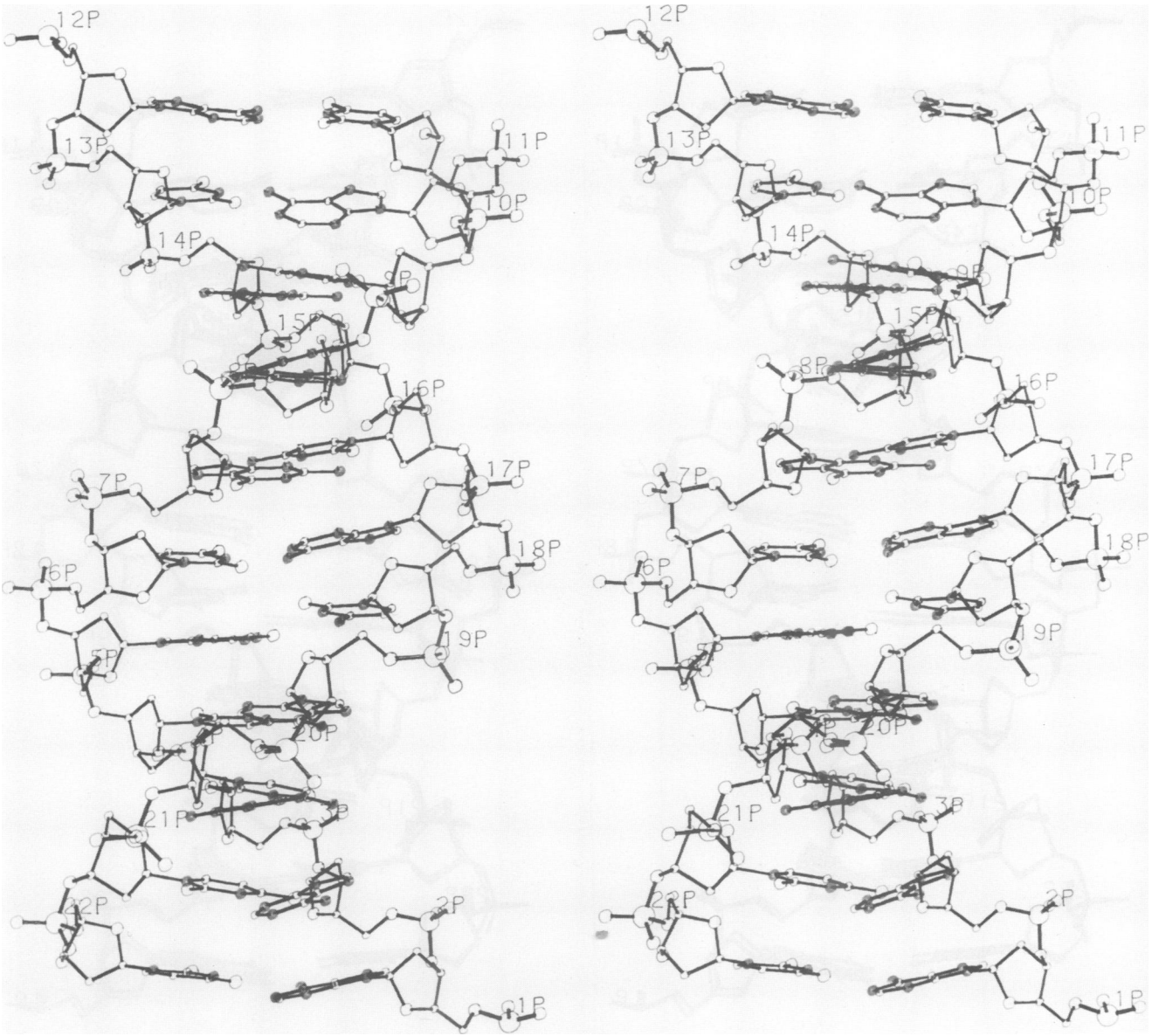

Fig. 2. Stereo view of refined structure I of the DNA undecamer. For the sake of clarity protons have been omitted.

computation of the three-dimensional structure using triangulation. This makes use of distance-geometry algorithms based on the interconvertability of intermolecular distances, torsion angles and cartesian coordinates providing the chirality of the structure is known (McKay, 1974; Crippen and Havel, 1978; Cohen and Sternberg, 1980; Braun *et al.*, 1981; Wüthrich *et al.*, 1982) and has been applied with some degree of success to a few small proteins (Braun *et al.*, 1983; Arseniev *et al.*, 1984). An alternative approach, and the one we have chosen, involves the refinement of an initial trial model derived either from a closely related structure or from model-building studies. The refinement technique used in this study, which has also been applied successfully to the refinement of the solution structure of the B-DNA hexamer 5′d (CGTACG)$_2$ (Clore *et al.*, 1985), is based on the restrained least square refinement program RESTRAIN (Haneef, 1983; Haneef *et al.*, 1984) and makes use solely of distance and planarity restraints.

The function minimized is given by

$$C = \Sigma W_d (d_t - d_c)^2 + \Sigma W_v |V| \quad (1)$$

where W_d and W_v are weighting coefficients, d_t and d_c are the target and calculated interatomic distances respectively, and $|V|$ is the determinant of the product-moment matrix V of planar groups of atoms given by

$$|V| = \begin{bmatrix} \Sigma x_i x_i & \Sigma x_i y_i & \Sigma x_i z_i \\ \Sigma y_i x_i & \Sigma y_i y_i & \Sigma y_i z_i \\ \Sigma z_i x_i & \Sigma z_i y_i & \Sigma z_i z_i \end{bmatrix} \quad (2)$$

(The necessary and sufficient condition for a set of atoms to be planar is that the determinant of the matrix V is zero.) The interatomic distances include all distances between covalently bonded atoms, between atoms defining fixed bond angles, and between atoms defining hydrogen bonding in the AT and GC base pairs, as well as the interproton distances determined from the pre-steady state NOE measurements. For each residue the C1′-atom of the deoxyribose and all the atoms of the base (with the exception of the methyl protons) are constrained to lie in the same plane.

Two refinements were carried out and in both cases the initial

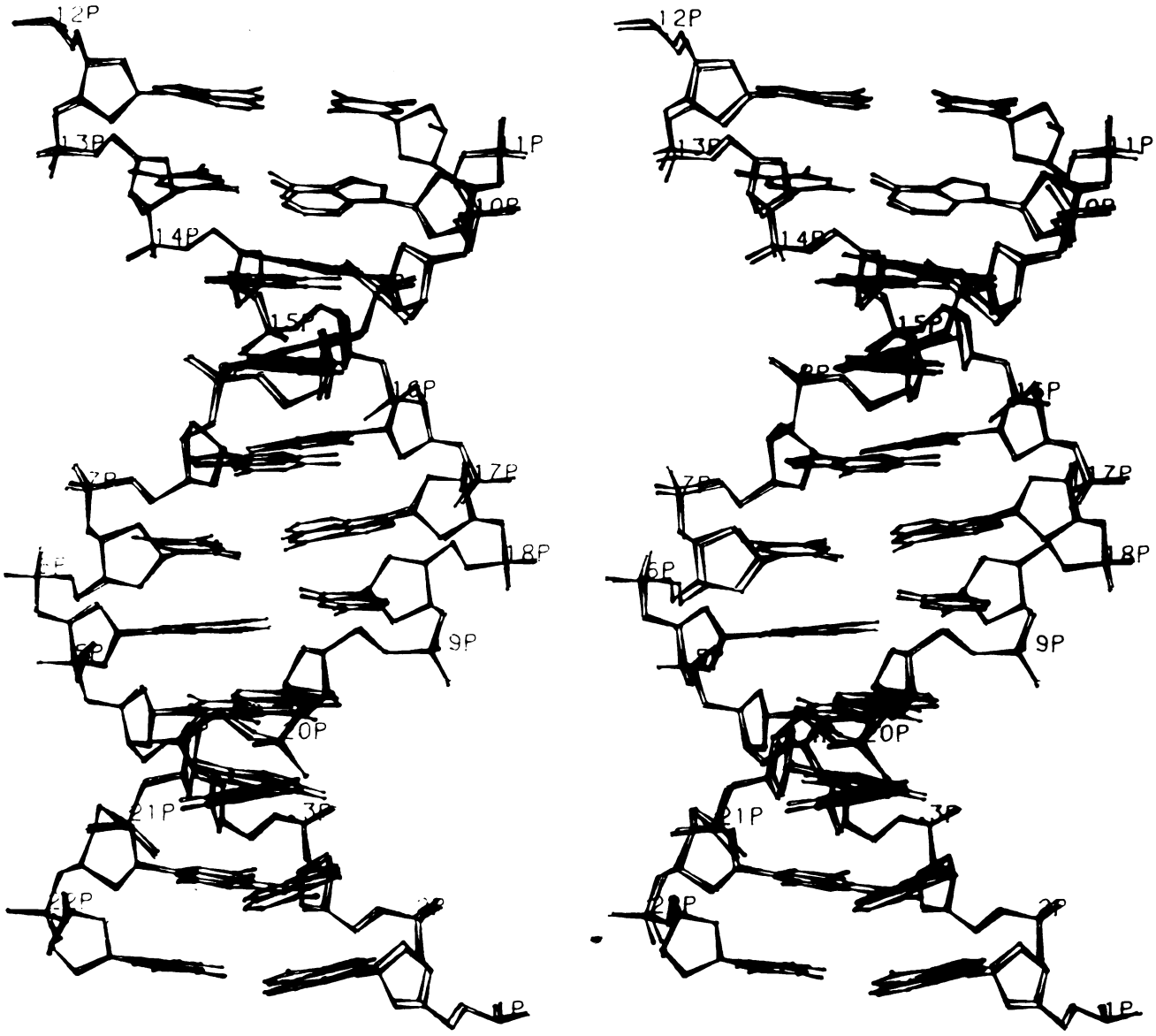

Fig. 3. Stereo view of refined structures I and II of the DNA undecamer superimposed. For the sake of clarity protons have been omitted.

input coordinates were those of classical B-DNA derived from the fibre diffraction data of Arnott and Hukins (1973). This starting structure is entirely reasonable as both CD (Martin *et al.*, 1984) and NOE (Clore and Gronenborn, 1984a, 1984c) data have shown that the structure of the undecamer in solution is that of right-handed B-DNA. In the first refinement which yielded structure I, the weightings for the three distance ranges, $r<2.12$ Å, 2.12 Å $<r<2.62$ Å and $r>2.62$ Å, and the planes, were applied in a ratio of 5:4:3:4 during the entire course of the refinement (comprising a total of 80 cycles). In the second refinement which resulted in structure II, the weights for the first 60 cycles were applied in a ratio of 10:10:7:7; this was followed by five cycles of regularization in which the interproton distances derived from the NMR measurements were excluded from the refinement; finally, a further 15 cycles were performed with the interproton distances reintroduced and the weight applied in a ratio of 5:4:3:4.

The RMS difference between the target and calculated values for the distance and planar restraints in the initial and final structures is given in Table I together with the overall RMS shift factors between the three structures. The average RMS differences in the coordinates of the sugar-phosphate and base moieties between the three structures are plotted as a function of residue number in Figure 1; a stereoview of structure I, viewed along the helix axis, is shown in Figure 2, and a stereoview of structures I and II superimposed is shown in Figure 3. It is clear from inspection of the data in Table I that the refinement has resulted in a considerable improvement in the agreement between calculated and target distance restraints. This is most marked in the case of the interproton distance restraints where the RMS difference for the refined structures I and II is 0.200 and 0.193 Å, respectively, which is comparable with the error in the experimental data (± 0.2 Å; Clore and Gronenborn 1984c, 1985), compared with a value of 0.642 Å for the initial classical B-DNA model. Examination of Table I and Figures 1 and 3 also reveals that the difference between the two refined structures I and II is negligible. This is further emphasized by the various conformational parameters given in Tables II and III.

Table II. Torsion and propellor twist angles for the refined structures I and II of the DNA undecamer

	Refined structure I/Refined Structure II									
	Glycosyl (°)	Main chain torsion angles (°)						Phosphorus atom separation (Å)	Propellor twist (°)	Sugar pucker
	χ	α	β	γ	δ	ϵ	ξ		ψ	
Strand 1										
A_1	−95/−96	−	−172/−175	51/53	133/128	163/163	−91/−88	6.59/6.71	12/10	C1′-exo
A_2	−78/−79	−38/−37	−148/−149	24/20	149/149	160/160	−91/−92	6.37/6.33	11/12	C2′-endo
G_3	−121/−125	−40/−37	−159/−163	20/18	115/108	152/145	−54/−42	6.33/6.33	17/19	C1′-exo
T_4	−122/−126	−68/−76	−155/−147	46/46	126/124	167/165	−83/−79	6.45/6.38	4/1	C1′-exo
G_5	−114/−117	−46/−45	−154/−154	20/16	126/122	143/133	−56/−42	6.28/6.30	8/12	C1′-exo
T_6	−121/−123	−69/−81	−158/−149	44/48	109/104	169/170	−73/−72	6.24/6.01	21/18	C1′-exo
G_7	−101/−107	−60/−61	−161/−165	44/48	147/139	168/165	−103/−99	6.58/6.64	0/5	C2′-endo
A_8	−115/−124	−41/−39	−163/−167	29/31	134/128	157/154	−71/−65	6.31/6.33	20/20	C1′-exo
C_9	−126/−132	−58/−63	−151/−145	38/39	132/128	158/154	−81/−75	6.49/6.33	5/0	C1′-exo
A_{10}	−104/−114	−61/−68	−150/−146	33/40	126/122	151/146	−61/−55	6.48/6.46	11/11	C1′-exo
T_{11}	−98/−99	−67/−76	−143/−139	45/50	160/160	−	−	−	1/0	C2′-endo
Strand 2										
A_{12}	−118/−113	−	−165/−165	27/17	112/113	148/141	−54/−44	6.61/6.59	1/0	C1′-exo
T_{13}	−96/−95	−62/−68	−148/−146	45/44	150/151	153/154	−96/−91	6.43/6.44	11/11	C2′-endo
G_{14}	−106/−102	−43/−48	−142/−130	30/22	138/140	144/137	−80/−70	6.32/6.22	5/0	C2′-endo
T_{15}	−121/−122	−51/−57	−160/−155	37/38	125/120	166/166	−73/−67	6.28/6.23	20/20	C1′-exo
C_{16}	−126/−125	−59/−65	−156/−156	45/49	133/133	177/178	−102/−105	6.73/6.77	0/5	C2′-endo
A_{17}	−120/−118	−44/−41	−164/−162	25/21	124/124	156/155	−62/−58	6.51/6.44	21/18	C1′-exo
C_{18}	−118/−117	−57/−58	−154/−155	27/27	111/108	150/144	−53/−44	6.31/6.27	8/12	C1′-exo
A_{19}	−124/−121	−70/−78	−149/−144	38/39	120/119	141/133	−59/−50	6.41/6.38	4/1	C1′-exo
C_{20}	−125/−124	−74/−86	−145/−137	45/50	119/117	152/153	−66/−65	6.19/6.15	17/19	C1′-exo
T_{21}	−115/−116	−71/−78	−155/−153	62/68	147/149	171/175	−118/−125	6.68/6.74	11/12	C2′-endo
T_{22}	−94/−93	−48/−49	−157/−158	42/41	160/162	−	−	−	12/10	C2′-endo
Mean	−113 ± 14	−61 ± 16	−153 ± 11	38 ± 14	129 ± 17	155 ± 13	−71 ± 23	6.42 ± 0.18	10 ± 7	C1′-exo
B_C-DNA[a]	−117 ± 14	−63 ± 8	171 ± 14	54 ± 8	123 ± 25	−169 ± 25	−108 ± 34	6.68 ± 0.23	13 ± 5	C1′-exo
B_F-DNA[b]	−98	−47	−146	36	156	155	−95	6.46		C2′-endo

The main chain torsion angles are defined by P^{α}- $05'^{\beta}$- $C5'^{\gamma}$- $C4'^{\delta}$- $C3'^{\epsilon}$- $O3'^{\xi}P$ and the glycosidic bond torsion angles by χ_{pur} = O1′ - C1′ - N9 - C4 and χ_{pyr} = O1′ - C1′ - N1 - C2, with zero at the eclipsed position and positive angles by clockwise rotation of the further pair of atoms. The propellor twist angle ψ is the dihedral angle between individual base planes.
[a]From the crystal data of Dickerson and Drew (1981) on the self-complementary B-DNA dodecamer 5′d $(CGCGAATTCGCG)_2$.
[b]From the fibre diffraction data of Arnott and Hukins (1973).

Table III. Rise per base pair (h) and local helical twist (t_1), base roll (θ_R) and base tilt (θ_t) angles for refined structures I and II of the DNA undecamer

	Refined structure I/Refined structure II							
			Strand 1			Strand 2		
Base pair step	t_1(°)	h(Å)	θ(°)	θ_R(°)	θ_t(°)	θ(°)	θ_R(°)	θ_t(°)
1. A_1T_{22}-A_2T_{21}	38/39	3.7/4.0	8/15	2/2	8/15	7/6	−5/−5	5/4
2. A_2T_{21}-G_3C_{20}	34/33	3.3/3.1	9/7	7/3	−5/−6	0/2	0/2	0/0
3. G_3C_{20}-T_4A_{19}	35/34	3.3/3.3	8/9	8/9	0/−2	3/3	−3/−3	0/1
4. T_4A_{19}-G_5C_{18}	34/35	3.3/3.3	11/15	−11/−15	1/2	4/1	−3/−1	−3/0
5. G_3C_{18}-T_6A_{17}	34/34	3.0/2.9	8/10	−6/−8	5/5	7/5	−5/−2	5/5
6. T_6A_{17}-G_7C_{16}	39/39	3.7/3.6	14/11	13/10	6/4	17/16	−17/−16	−2/1
7. G_7C_{16}-A_8T_{15}	32/31	3.5/3.5	9/10	−7/−8	−6/−5	5/5	5/5	0/0
8. A_8T_{15}-C_9G_{14}	33/34	2.9/2.9	6/5	0/−1	−6/−5	15/18	−25/−17	2/4
9. C_9G_{14}-$A_{10}T_{13}$	38/38	3.5/3.4	16/17	−7/−13	14/10	6/6	−1/0	−6/−6
10. $A_{10}T_{13}$-$T_{11}A_{12}$	30/30	3.7/3.8	15/10	15/10	−2/0	5/6	0/−2	5/6
Mean	35 ± 3	3.4 ± 0.3	11 ± 4	0.2 ± 9	1.7 ± 7	7 ± 5	−4.2 ± 7	1.2 ± 3.5
B_C-DNA[a]	37.3 ± 3.8	3.33 ± 0.13						
B_F-DNA[b]	36	3.4						

The base roll angle θ_R is the rotation about an axis in the plane of the bases perpendicular to the pseudo-dyad and is positive when opening towards the minor groove. The base tilt angle θ_t is the rotation about the pseudo-dyad axis passing through the base plane and is positive when opening to the outside of the molecule. θ is the magnitude of the total angle between successive base plane normals and is given by $\sin^{-1}[(\sin^2\theta_R + \sin^2\theta_t)^{1/2}]$.
[a]From the crystal data of Dickerson and Drew (1981).
[b]From the fibre diffraction data of Arnott and Hukins (1973).

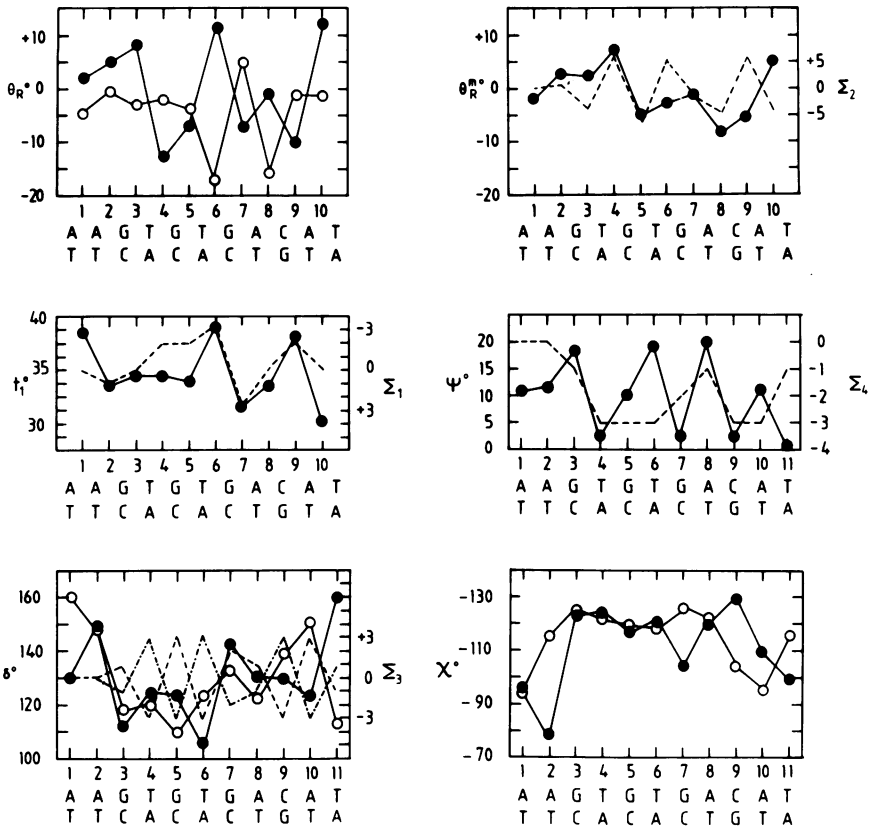

Fig. 4. Variations in base roll angles θ_R (●, strand 1; ○, strand 2), mean base roll angles θ_R^m, helix twist angles, t_1, propellor twist angles ψ, C4-C3′ bond torsion angles δ (●, strand 1; ○, strand 2) and glycosidic bond torsion angles χ (●, strand 1; ○, strand 2) as a function of residue for the refined structures of the DNA undecamer. Angle values plotted are the average of those for refined structures I and II. In addition the variations in the sum functions Σ (---) defined by Dickerson (1983) are also plotted. Σ_1 is the sum function for helical twist, Σ_2 for base roll, Σ_3 for the C4′-C3′ bond torsion angle (---, strand 1; -·-·-, strand 2) and Σ_4 for propellor twist. The terms for Σ_1 are +1, −2, +1 for x-Pur-Pyr-x and +2, −4, +2 for x-Pyr-Pur-x; for Σ_2, +1, −2, +1 for x-Pur-Pyr-x and −2, +4, −2 for x-Pyr-Pur-x; for Σ_3, +1, −1 for Pur-Pyr and −2, +2 for Pyr-Pur; and for Σ_4, −1, −1 for Pur-Pyr and −2, −2 for Pyr-Pur.

The nature of the refined structures

For the following discussion it is essential to bear in mind that the interproton distances measured by NMR are not arithmetic means but $(<r^{-6}>)^{-1/6}$ means. This has certain important consequences as the undecamer in solution is a dynamic rather than a static structure and possesses internal mobility (Clore and Gronenborn, 1984b). Consequently, the measured interproton distances are heavily weighted towards fluctuations with the shortest interproton distances, a feature which could potentially result in a distorted refined structure. Fortunately, the refinement itself provides information concerning both the magnitudes of the internal motions and the quality of the refined structure as a representation of the 'true' solution structure. This is due to two factors: (i) a large number (150) of interproton distances are used in the refinement, and (ii) many of these distances are correlated (e.g., for three adjacent residues i−1, i and i+1, all intra- and internucleotide interproton distances will be interdependent). Thus, if the magnitude of the internal motions is large, a single structure would not be able to provide an acceptable fit to the experimental data. In the present case, it is clear that the magnitude of the internal motions must be small in order to accommodate an overall RMS difference of only 0.2 Å between the experimental and calculated interproton distances for refined structures I and II. We therefore conclude that refined structures I and II are good representations of the solution structure of the undecamer and that the small differences between the two refined structures provides a measure of the error in the refined coordinates.

Local structural variations

Although the overall structure of the undecamer is that of B-DNA it can be seen from the data in Tables II and III that there are very large variations in the values of the various conformational parameters describing the structure of the undecamer. This is depicted graphically in Figure 4 for the base-roll (θ_R), helical twist (t_1) and propellor twist (ψ) angles and for the C4′-C3′ (δ) and glycosidic (χ) bond torsion angles. The magnitude of these variations is comparable with that observed in the crystal structure of the B-DNA dodecamer 5′d $(CGCGAATTCGCG)_2$ (Dickerson and Drew, 1981) and considerably larger than that observed in the refined solution structure of the B-DNA hexamer 5′d $(CGTACG)_2$ (Clore *et al.*, 1985).

Recently Dickerson (1983) proposed a series of simple sum functions based on Calladine's principles (1982) to predict the dependence of variations in the values of θ_R, t_1, ψ and δ on sequence. These sum functions are also plotted as a function of residue in Figure 4. In the case of the crystal structure of the B-DNA dodecamer 5′d $(CGCGAATTCGCG)_2$ the measure of agreement between observed and predicted variations was reasonable (Dickerson, 1983). In the case of the undecamer, however, the situation is somewhat different. The prediction is quite good for the variations in the mean base roll angles (θ_R^m) but poor for the variations in the propellor twist angles (ψ) and

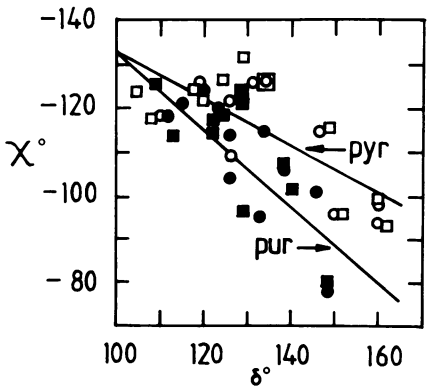

Fig. 5. Correlation of glycosidic χ and C4′-C3′ δ bond torsion angles. Symbols: ● and ■, purine residues of refined structures I and II respectively; ○ and □, pyrimidine residues of refined structures I and II respectively. The linear regression lines (—) for the purine and pyrimidine residues are also shown.

the C4′-C3′ bond torsion angles (δ). In addition, the observed variations in the helical twist angles (t_1) are almostly exactly the opposite to those predicted by the sum functions Σ_1: a negative value of Σ_1 should represent a decrease in t_1 and a positive value in an increase (Dickerson, 1983) whereas exactly the opposite is found for the undecamer. This poor measure of agreement between observed and predicted variations is not entirely surprising. Firstly, the database from which the predictions were derived is small; secondly, the contributions to the sum functions arise only from Pyr-Pur and Pur-Pyr steps and no distinction is made between the types of pyrimidine and purine residues; and thirdly, only nearest neighbour interactions are considered.

Despite the poor agreement between observed and predicted variations in δ, the correlation between C4′-C3′ (δ) and glycosidic (χ) bond torsion angles observed in the crystal structure of the B-DNA dodecamer (Dickerson and Drew, 1981) is also observed for the undecamer (Figure 5), and the principle of anticorrelation, in which the pyrimidine residue of a given base pair has a lower value of δ than the purine residue, is seen to hold for base pairs 2, 5, 6, 7, 8 and 9 (Figure 4). Where this principle is not followed, the difference in δ values is either not significant as in the case of base pairs 3 and 4 or can be attributed to distortions arising from end effects as in the cse of base pairs 1, 10 and 11. In addition, we find that for a given value of χ, the value of δ is likely to behigher for a pyrimidine than a purine residue.

Conclusion

Here we have presented the refined solution structure of a DNA undecamer comprising the specific target site for the cAMP receptor protein in the *gal* operon. It is clear that although the overall B-DNA framework is maintained, the structure in solution is far from regular. For example, propellor twist angles range from 20° to 0°, helical twist angles from 39° to 30°, base roll angles from −25° to +15°, and so on. This should have important consequences for specific DNA-protein interactions as they most likely involve recognition not only of sequence but also of structure. What also emerges from the present study is that the rules governing structural variations are not quite as simple as those derived on the basis of the crystal structure of the B-DNA dodecamer 5′d $(CGCGAATTCGCG)_2$ (Dickerson and Drew, 1981). Given that so few B-type oligonucleotide structures have been solved to date either in the crystal state or in solution, it is too early as yet to safely generalize the pattern of local structural variations observed for one DNA oligonucleotide to others.

References

Arnott,S. and Hukins,D.W.L. (1973) *J. Mol. Biol.*, **81**, 93-105.
Arseniev,S.A., Kondakov,V.I., Maiorov,V.N. and Bystrov,V.F. (1984) *FEBS Lett.*, **165**, 57-62.
Braun,W., Bösch,C., Brown,C.R., Go,N. and Wüthrich,K. (1981) *Biochim. Biophys. Acta*, **667**, 377-396.
Braun,W., Wider,G., Lee,K.H. and Wüthrich,K. (1983) *J. Mol. Biol.*, **169**, 921-948.
Calladine,C.R. (1982) *J. Mol. Biol.*, **161**, 343-352.
Clore,G.M. and Gronenborn,A.M. (1983) *EMBO J.*, **2**, 2109-2115.
Clore,G.M. and Gronenborn,A.M. (1984a) *Eur. J. Biochem.*, **141**, 119-129.
Clore,G.M. and Gronenborn,A.M. (1984b) *FEBS Lett.*, **172**, 219-225.
Clore,G.M. and Gronenborn,A.M. (1984c) *FEBS Lett.*, **175**, 117-123.
Clore,G.M. and Gronenborn,A.M. (1985) *J. Magn. Resonance*, **61**, 158-164.
Clore,G.M., Lauble,H., Frenkiel,T.A. and Gronenborn,A.M. (1984) *Eur. J. Biochem.*, **145**, 629-636.
Clore,G.M., Gronenborn,A.M., Moss,D.S. and Tickle,I.J. (1985) *J. Mol. Biol.*, in press.
Cohen,F.E. and Sternberg,M.J.E. (1980) *J. Mol. Biol.*, **138**, 321-333.
Crippen,G.M. and Havel,T.F. (1978) *Acta Crystallogr.*, **A34**, 282-284.
Dickerson,R.E. (1983) *J. Mol. Biol.*, **166**, 419-441.
Dickerson,R.E. and Drew,H.R. (1981) *J. Mol. Biol.*, **149**, 761-786.
Dobson,C.M., Olejniczak,E.T., Poulsen,F.M. and Ratcliffe,R.G. (1982) *J. Magn. Resonance*, **48**, 87-110.
Ebright,R.H. (1982) in Griffen,J. and Duax,W. (eds.), *Molecular Structure and Biological Function*, Elsevier North-Holland, Amsterdam, pp. 99-110.
Feigon,J., Leupin,W., Denny,W.A. and Kearns,D.R. (1983) *Biochemistry (Wash.)*, **22**, 5943-5951.
Gronenborn,A.M., Clore,G.M. and Kimber,B.J. (1984) *Biochem. J.*, **221**, 723-736.
Gronenborn,A.M. and Clore,G.M. (1984) *Progr. Nucl. Magn. Reson. Spectr.*, in press.
Haneef,I. (1983) *RESTRAIN User Guide*, published by Birkbeck College, London.
Haneef,I., Moss,D.S., Stanford,M.J. and Borkoti,N. (1984) *Acta Crystallogr. A*, in press.
Haasnoot,C.A.G., Westerink,N.P., van der Marel,G.A. and van Boom,J.H. (1983) *J. Biomol. Struct. Dyn.*, **1**, 131-149.
Hare,D.R., Wemmer,D.E., Chou,S.H., Drobny,G. and Reid,B.R. (1983) *J. Mol. Biol.*, **171**, 319-336.
Keepers,J.W. and James,T.L. (1984) *J. Magn. Resonance*, **53**, 104-124.
Martin,S.R., Gronenborn,A.M. and Clore,G.M. (1983) *FEBS Lett.*, **159**, 102-106.
McKay,A.L. (1974) *Acta Crystallogr.*, **A30**, 440-447.
Reid,D.G., Salisbury,S.A., Rellard,S., Zhakhed,Z. and Williams,D.H. (1983a) *Biochemistry (Wash.)*, **22**, 2019-2025.
Reid,D.G., Salisbury,S.A., Brown,T., Williams,D.H., Vasseur,J.J., Rayner,B. and Imbach,J.L. (1983b) *Eur. J. Biochem.*, **135**, 307-314.
Scheek,R.M., Boelens,R., Russo,N., van Boom,J.H. and Kaptein,R. (1984) *Biochemistry (Wash.)*, **23**, 1371-1376.
Strop,P., Wider,G. and Wüthrich,K. (1983) *J. Mol. Biol.*, **166**, 641-667.
Taniguchi,T., O'Neill,M.C. and de Crombrugghe,B. (1979) *Proc. Natl. Acad. Sci. USA*, **76**, 5090-5094.
Wagner,G. and Wüthrich,K. (1979) *J. Magn. Resonance*, **33**, 675-680.
Wagner,G. and Wüthrich,K. (1982a) *J. Mol. Biol.*, **159**, 347-366.
Wagner,G. and Wüthrich,K. (1982b) *J. Mol. Biol.*, **160**, 334-361.
Wagner,G., Kumar,A. and Wüthrich,K. (1981) *Eur. J. Biochem.*, **114**, 375-384.
Weiss,M.A., Patel,D.J., Sauer,R.T. and Karplus,M. (1984) *Proc. Natl. Acad. Sci. USA*, **81**, 130-134.
Williamson,M.P., Marion,D. and Wüthrich,K. (1984) *J. Mol. Biol.*, **173**, 341-359.
Wüthrich,K., Wider,G., Wagner,G. and Braun,W. (1982) *J. Mol. Biol.*, **155**, 311-319.

Received on 30 November 1984